

# Constraints on CPT violation from WMAP three year polarization data: a wavelet analysis

Paolo Cabella<sup>a,\*</sup>, Paolo Natoli<sup>b,†</sup> and Joseph Silk<sup>a,‡</sup>

<sup>a</sup> *University of Oxford, Astrophysics, Keble Road, Oxford, OX1 3RH, U.K. and*

<sup>b</sup> *Dipartimento di Fisica e sezione INFN, Università di Roma “Tor Vergata”,  
Via della Ricerca Scientifica, I-00133 Roma, Italy*

We perform a wavelet analysis of the temperature and polarization maps of the Cosmic Microwave Background (CMB) delivered by the WMAP experiment in search for a parity violating signal. Such a signal could be seeded by new physics beyond the standard model, for which the Lorentz and  $\mathcal{CPT}$  symmetries may not hold. Under these circumstances, the linear polarization direction of a CMB photon may get rotated during its cosmological journey, a phenomenon also called cosmological birefringence. Recently, Feng et al. have analyzed a subset the WMAP and BOOMERanG 2003 angular power spectra of the CMB, deriving a constraint that mildly favors a non zero rotation. By using wavelet transforms we set a tighter limit on the CMB photon rotation angle  $\Delta\alpha = -2.5 \pm 3.0$  ( $\Delta\alpha = -2.5 \pm 6.0$ ) at the one (two)  $\sigma$  level, consistent with a null detection.

## I. INTRODUCTION

The CMB is one of the primary experimental windows to the early universe. Recent observations have reached remarkable precision. When combined with other complementary cosmological datasets, the WMAP three year (hereafter, WMAP3) observations [1] convincingly support the so-called standard model of structure formation [2]. However the CMB may provide further information. In principle, one may use the background photons to constrain new physics beyond “standard” models. A positive answer might be provided by the study of CMB polarization (CMBP), whose observations currently mark the experimental frontier of the field. Pioneering observations, including DASI [3], CBI [4], BOOMERanG 2003 [5] (hereafter B03), MAXIPOL [6], and WMAP itself [7] have yielded detections of the CMBP over a wide range of angular scales. Within the next decade, ground or space-based experiments may detect via the CMBP a signal from primordial gravitational waves [8], thus constraining the energy scale of the inflation and probing particle physics well beyond the capability of any conceivable terrestrial accelerator. The CMBP can also provide information on symmetry-violating physics beyond the Lee-Yang parity ( $\mathcal{P}$ ) breaking that is central to the standard model, yet not observable through CMB anisotropies due to their charge blind character. In general, the breakdown of spacetime symmetries is a potential tracer of new physics [9]. Several models exist that predict non-standard  $\mathcal{P}$  and  $\mathcal{CP}$  violations ( $\mathcal{C}$  standing for charge conjugation), as well as  $\mathcal{CPT}$  violations ( $\mathcal{T}$  being time reversal) and the related (through the anti- $\mathcal{CPT}$  theorem [10]) breakdown of Lorentz invariance. A number of tests have been suggested and (in many cases) performed, either in terrestrial and orbital laboratories [11] or through cosmological observations [12, 13]. These violations might also have a measurable imprint on the observed CMBP pattern, whose statistical properties are constrained by the assumption of symmetry conservation.

For a sky direction  $\hat{n}$ , a polarized map of the CMB is usually given in terms of total intensity (or temperature)  $T(\hat{n})$  and linear polarization Stokes parameters  $Q(\hat{n})$  and  $U(\hat{n})$ . The  $T$  field can be decomposed into scalar (S) spherical harmonics  $Y_{lm}(\hat{n})$ , obtaining the coefficients  $a_{lm}^T$ .  $Q$  and  $U$  are components of a symmetric, trace-free rank 2 tensor, and are expanded in tensor spherical harmonics  $Y_{lm}^G(\hat{n})$  and  $Y_{lm}^C(\hat{n})$  with coefficients  $a_{lm}^G$  and  $a_{lm}^C$ , respectively. These correspond to scalar (gradient-like) ‘G’ and pseudo-scalar (curl-like) ‘C’ modes [8]. Under hypothesis of Gaussianity and isotropy, the statistical properties the CMB are described by two point correlation functions on the sphere, whose Legendre transforms define six angular power spectra:  $C_l^{ZZ'} = \langle a_{lm}^Z (a_{lm}^{Z'})^* \rangle$  with  $Z, Z' = \{T, G, C\}$ . If the physics controlling CMB fluctuations is parity conserving the cross spectra  $C_l^{TC}$  and  $C_l^{GC}$  must vanish due to the different handedness of the C and (S,G) harmonics. Therefore, if the standard cosmological model holds, we should expect no relevant information from  $TC$  and  $GC$ . On the other hand, detection of non-zero primordial  $TC$  and/or  $GC$  may probe fundamental physics in the early universe, such as the presence of a primordial homogeneous [14] or helical [15] magnetic field which would induce Faraday rotation and non-zero  $TC$  correlations. Parity-asymmetric gravity dynamics during inflation may generate a discrepancy among left and right-handed gravitational waves, so

\*Electronic address: cabella@astro.ox.ac.uk

†Electronic address: paolo.natoli@roma2.infn.it

‡Electronic address: silk@astro.ox.ac.uk

that  $TC$  and  $GC$  are non-zero [16]. Particle physics models with non-standard parity-violating interactions also predict non-vanishing  $TC$  and  $CG$  signals [17].

In this paper we focus on a class of models that exhibit parity violations in the photon sector. A Chern-Simons term is introduced in the effective Lagrangian [13]:

$$\Delta\mathcal{L} = -\frac{1}{4}p_\mu\epsilon^{\mu\nu\rho\sigma}F_{\rho\sigma}A_\nu,$$

where  $F^{\mu\nu}$  is the Maxwell tensor and  $A^\mu$  the 4-potential. The 4-vector  $p_\mu$  may be interpreted as the derivative of the quintessence field or the gradient of a function of the Ricci scalar [18]. In either case a  $\mathcal{P}$  violation always arises provided that  $p_0$  is non-zero, while  $\mathcal{C}$  and  $\mathcal{T}$  remain intact. Hence,  $\mathcal{CP}$  and  $\mathcal{CPT}$  symmetries are also violated, as well as Lorentz invariance, since  $p^\mu$  picks up a preferred direction in space-time. The net effect on a propagating photon is to rotate its polarization direction by an angle  $\Delta\alpha$ , hence the name “cosmological birefringence”. Historically, the effect has been constrained by measuring polarized light from high redshift radio galaxies and quasars [13, 19]. Obviously, the CMB photons would also be affected and, due to their longer journey, may get a larger rotation. A consequence for the CMB pattern is the mixing of  $G$  and  $C$  modes: the  $TG$  and  $GC$  correlations still vanish at last scattering surface, but the observable CMB spectra are distorted as [16, 20]:

$$C_l'^{TC} = C_l^{TG} \sin 2\Delta\alpha \quad (1)$$

$$C_l'^{GC} = \frac{1}{2}(C_l^{GG} - C_l^{CC}) \sin 4\Delta\alpha \quad (2)$$

$$C_l'^{TG} = C_l^{TG} \cos 2\Delta\alpha \quad (3)$$

$$C_l'^{GG} = C_l^{GG} \cos^2 2\Delta\alpha + C_l^{CC} \sin^2 2\Delta\alpha \quad (4)$$

$$C_l'^{CC} = C_l^{CC} \cos^2 2\Delta\alpha + C_l^{GG} \sin^2 2\Delta\alpha. \quad (5)$$

where the primed quantities are rotated. In [21], the  $TT$  and  $TG$  power spectra measured by WMAP3 together with all six spectra measured by B03 have been used to perform a global fit, yielding a mild detection for a non zero rotation (but see also [24] for a similar analysis restricted to the B03 power spectra and [25] where constraints on the coupling between the quintessence and the pseudoscalar of electromagnetism are derived, based again on B03 data). Using the same data set, a similar result has been found in [22], and used to constrain a specific baryo/leptogenesis model, while an interaction between the neutrino asymmetry and a term Chern-Simons term has been proposed in [23] as a possible explanation for the result found [21]. Forecasted constraints on  $\Delta\alpha$  for high sensitivity experiments such as Planck or CMBpol can be found in [26].

Here we constrain  $\Delta\alpha$  with a wavelet analysis. A rotation of the photon polarization direction leaves an imprint on each resolution element (or pixel) of the Q and U maps, and a map-based estimator appears appropriate. Wavelets are a natural choice because they allow for multi-scale pixel analysis. We compute the wavelet cross-correlation coefficients for  $TC$  and  $GC$  to build a goodness of fit estimator that we apply to the WMAP3  $\{T, Q, U\}$  maps. Our analysis is complementary to that of [21], where the information for  $TC$  and  $GC$  comes from B03. The two analyses differ in the method and (substantially) in the data set (the only overlap being the WMAP3 temperature map). In the following, we derive more stringent limits on  $\Delta\alpha$  by adapting the wavelet formalism to tackle polarization, a point that has not been addressed to date in the CMB literature.

The plan of the paper is as follows: in section II we describe our wavelet based method to constrain  $\Delta\alpha$ : section III we define a suitable estimator and apply it to WMAP3 data, making use of numerical simulations. Finally in section IV we draw our conclusions.

## II. A WAVELET STATISTIC FOR TEMPERATURE AND POLARIZATION

Given a position  $\vec{X}$ , wavelets are filter functions  $\Psi(\vec{X}; b, R)$  that also depend on a characteristic scale  $R$  and translation  $b$ . They provide scale-varying transforms that remain localized in pixel space. Moreover, they consist of an infinite set of basis functions, thus providing some freedom of choice in matching their functional form to the target signal. Several authors have exploited this flexibility as a powerful tool in CMB data analysis. Wavelets have been used for denoising [27], point source extraction [28], foreground removal [29] and for detecting the integrated Sachs Wolfe effect [30]. Since the wavelet transform preserves linearity, its coefficients can be used to constrain the statistics of the field at different scales. In particular, the spherical Mexican hat wavelet (SMHW) has been used to flag statistical anomalies in the WMAP data [31] and to constrain primordial non-Gaussianity [32] (other types of wavelets have been shown to be sensitive to yet different anomalies, e.g. [33]). SMHW are generated from ordinary MH wavelets through a stereographic projection on the tangent plane [34] that is known to preserve their basic properties

[35]. The SMHW is defined as:

$$\Psi(y, R) = \frac{1}{\sqrt{2\pi}N(R)} \left[ 1 + \left( \frac{y}{2} \right)^2 \right]^2 \left[ 2 - \left( \frac{y}{R} \right)^2 e^{-y^2/2R^2} \right]$$

where  $y = 2 \tan \theta/2$  ( $\theta$  is the polar angle),  $R$  is the scale of convolution, and  $N(R)$  a normalization factor. For a T map, the wavelets coefficients are:

$$W^T(R, \hat{n}) = \int d\Omega' T(\hat{n} + \hat{n}') \Psi(\theta', R) .$$

This convolution can be performed in harmonic space:

$$W(R, \hat{n}) = \sum_{lm} \left( \frac{4\pi}{2l+1} \right)^{1/2} a_{lm}^T \Psi_l(R) Y_{lm}(\hat{n}) \quad (6)$$

where  $\Psi_l(R)$  are the Legendre expansion coefficients of the SMHW. Handling polarization requires more care, since  $Q$  and  $U$  are not rotationally invariant, being components of the rank 2 tensor  $P_{ab}$  [8]. By taking the covariant derivatives of  $P_{ab}$ , one can build two quantities that are rotational invariant and hence decomposed by S harmonics. This leads, again, to the  $G$  and  $C$  coefficients:

$$\begin{aligned} a_{lm}^G &= N_l \int d\Omega P_{ab}^{':ab}(\hat{n}) Y_{lm}^*(\hat{n}) \\ a_{lm}^C &= N_l \int d\Omega P_{ab}^{':ac}(\hat{n}) \epsilon_c^b(\hat{n}) Y_{lm}^*(\hat{n}). \end{aligned}$$

Here  $'\cdot'$  stands for the covariant derivatives on the sphere,  $\epsilon$  is the Levi-Civita trace-free antisymmetric tensor and  $N_l$  a normalization factor [8]. We similarly define SMHW coefficients as:

$$\begin{aligned} W^G(\hat{n}, R) &= \int d\Omega' P_{ab}^{':ab}(\hat{n} + \hat{n}') \Psi(\theta', R) \\ W^C(\hat{n}, R) &= \int d\Omega' P_{ab}^{':ac}(\hat{n} + \hat{n}') \epsilon_c^b(\hat{n} + \hat{n}') \Psi(\theta', R) . \end{aligned}$$

Note that we never explicitly compute derivatives, since the integrals can be performed in harmonic space (c.f. 6), provided we divide out the factor  $N_l$ . Finally, we consider the pixel-pixel cross correlation of the SMHW coefficients as our main statistic:

$$X^{ZC}(R) = \frac{1}{V} \int W^Z(\hat{n}, R) W^C(\hat{n}, R) d\hat{n} \quad (7)$$

where  $Z = \{T, G\}$  and  $V$  is a volume normalization that can be taken to be proportional to the total number of pixels  $N_p$ . The quantities in eq. 7 possess the same P symmetry of the usual harmonic cross spectra: they can be non-zero only if parity conservation is violated.

### III. NUMERICAL SIMULATIONS AND RESULTS

To constrain  $\Delta\alpha$ , the following scheme was employed. We modified the Healpix package [36] to generate a set of Monte Carlo (MC) simulations for  $\{T, Q, U\}$  maps containing a CMB signal whose polarization pattern is rotated according to eqs. 1-5; we use the WMAP3 best fit model as the (unrotated) fiducial angular power spectrum. The signal maps were smoothed according to the WMAP3 optical transfer function. We also simulated noise maps consistent with the WMAP3 instrumental properties. We add to each signal map a noise realization consistent with the WMAP3 instrumental properties. Simulating noise in TQU maps is more complicated than for T only, because the noise values of different Stokes parameters within a given pixel are usually correlated. For WMAP3,  $T$  is very weakly correlated with  $Q$  and  $U$ , so this coupling can be safely neglected [37]. On the contrary, in order to obtain accurate results one has to take into account the correlations between  $Q$  and  $U$ . The WMAP team has released  $2 \times 2$  effective hits arrays (hereafter,  $N_{\text{obs}}$  where the off diagonal elements represent the  $\langle QU \rangle$  inter pixel correlation (off pixel correlations are very weak and can be neglected); these matrices are given for each differential assembly (DA)

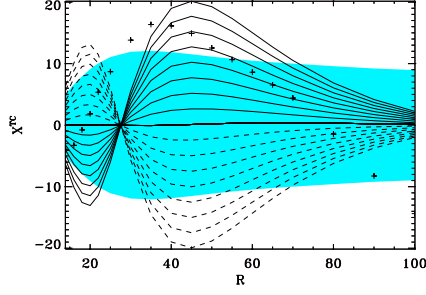


FIG. 1: MC means for  $X^{TC}$  (see text), for  $-8^\circ \leq \Delta\alpha \leq 8^\circ$ , step of  $1^\circ$  (dashed lines refer to positive  $\Delta\alpha$ , the middle line is for  $\Delta\alpha = 0$ , i.e.  $\mathcal{P}$  is conserved). The scale  $R$  is given in arcminutes. The shaded region shows the  $1\sigma$  range for  $\Delta\alpha = 0$ . Experimental points (WMAP3) are shown as crosses.

and for each observation year. To simulate noise maps, the following scheme is employed: for a given DA and for each pixel, we add the  $\mathbf{N}_{\text{obs}}$  arrays for different years. The three year, noise maps for each DA  $i$  are then simulated as:

$$\begin{pmatrix} Q_{i,p} \\ U_{i,p} \end{pmatrix} = \mathbf{N}_{\text{obs}}^{-1/2}(i,p) \sigma_{QU}(i) \quad (8)$$

where  $p$  identifies a given pixel,  $\sigma_{QU}$  is the nominal DA polarization sensitivity, as provided by the WMAP team [37] and  $\mathbf{N}_{\text{obs}}^{1/2}$  is the Choleski factor of  $\mathbf{N}_{\text{obs}}$ . The resulting noise plus signal maps for each DA are then weighted averaged to form a combined map comprising all DA's in the Q,V and W bands:

$$\begin{pmatrix} Q_p \\ U_p \end{pmatrix} = \left[ \sum_i^{N_{DA}} \mathbf{C}_{ip}^{-1} \right]^{-1} \sum_i^{N_{DA}} \mathbf{C}_{ip}^{-1} \begin{pmatrix} Q_{ip} \\ U_{ip} \end{pmatrix} \quad (9)$$

The combined map for  $T$  is computed by using the standard, scalar version of the procedure above:

$$T_p = \sum_i^{N_{DA}} \frac{T_{ip}}{\sigma_i^2} \left[ \sum_i \frac{1}{\sigma_i^2} \right]^{-1}. \quad (10)$$

To minimize residual foreground contamination we chose to use a rather conservative mask, the intersection of the Kp0 and P02 sky cuts [1]. The masked maps are downgraded in resolution to  $13.6'$ . We then compute the wavelet coefficients  $W^Z(p, R)$  (where  $Z = \{T, G, C\}$ ) over the discretized sphere. We consider 17 wavelet scales from  $14'$  to  $100'$ .<sup>1</sup> To avoid boundary effects, we widen the sky map up to a fraction  $2.5 R$  [31, 32]. Finally, we consider the goodness of fit statistics  $\chi^2(\Delta\alpha) = Y^T \mathbf{C}_{\Delta\alpha}^{-1} Y$ , where  $Y = X^{\text{WMAP}} - \bar{X}(\Delta\alpha)$ .  $X^{\text{WMAP}}$  is computed over the Q+V+W foreground-cleaned, optimally-weighted data map, while the mean (barred) quantities are derived from  $\sim 2000$  MC simulations. The covariance matrix  $\mathbf{C}_{\Delta\alpha}$  is estimated over a fresh set of simulations ( $\sim 4000$ ).

In fig. 1 we show, as a function of  $R$ , the MC mean values for  $X^{TC}$ , for  $-8^\circ \leq \Delta\alpha \leq 8^\circ$  with a step of  $1^\circ$ . The crosses are experimental points from WMAP3 and the shaded region is the  $1\sigma$  range, centered about the  $\Delta\alpha = 0$  case. In fig. 2 we show the same for  $X^{GC}$ , with the means in the range  $-16^\circ \leq \Delta\alpha \leq 16^\circ$  with a step of  $2^\circ$ . As expected for WMAP3,  $TC$  has a significantly larger signal to noise than  $GC$ . The means are computed over noisy simulations, but closely reproduce the ensemble predictions that can be derived from eq. 7. To show that our estimator is unbiased, we simulated a further MC set with given  $\Delta\alpha$  and checked that the means of the  $\chi^2$  estimates reproduce the input values with high accuracy. Throughout our analysis, we keep the dependence of  $\Delta\alpha$  in the estimator's covariance matrix (but find no significant change in our results if we drop this dependence: for WMAP3, our estimator's covariance is completely dominated by noise).

In fig. 3 we show the likelihoods of WMAP3 data for  $TC$  and  $GC$ .  $GC$  contributes very weakly to the joint likelihood  $\mathcal{L} \propto \exp(-\chi^2/2)$ . We estimate  $\Delta\alpha = -2.5 \pm 3.0$  and  $\Delta\alpha = -2.5 \pm 6.0$  at  $1\sigma$  and  $2\sigma$  confidence limit respectively. Thus, we find no evidence of parity violation from the WMAP3 data. These limits are slightly tighter

<sup>1</sup> The exact set of scales considered is  $R = [14, 16, 18, 20, 22, 25, 30, 35, 40, 45, 50, 55, 60, 65, 70, 80, 90, 100]$  arcmin.

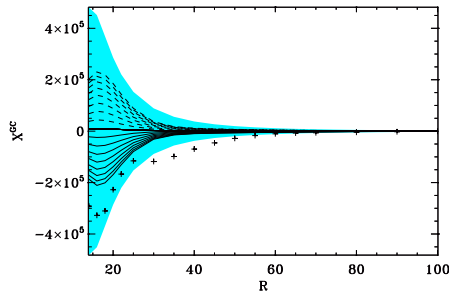


FIG. 2: Same as fig. 1 but for  $X^{GC}$  and  $-16^\circ \leq \Delta\alpha \leq 16^\circ$ , step of  $2^\circ$ . Note the lower signal to noise.

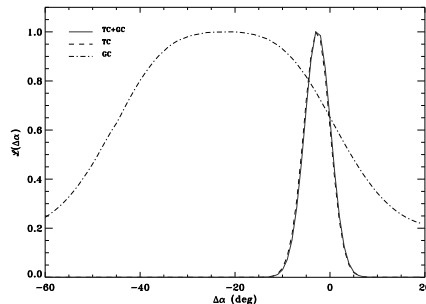


FIG. 3: Likelihood functions of the cosmological birefringence angle  $\Delta\alpha$  for CG (dotted) and TC (dashed), computed from the wavelet estimator on WMAP3 data. The solid (blue) line is the global, covariance weighted, likelihood

than those given in [21], where a marginal detection for a non-zero  $\Delta\alpha$  is claimed and seems to be driven by the GC B03 data. To show that our conclusions do not depend on the particular fiducial power spectrum chosen (provided it is reasonable), we have allowed the latter to vary between the  $\pm 1\sigma$  experimental limits set by WMAP3, finding fully consistent results (no detection, very similar limits). This procedure extends to polarization the test suggested by [31] for temperature data.

As a further consistency check, we compared our estimator with a similar one, built using the angular power spectrum rather than wavelets. In the case of pure signal, under the assumption of Gaussianity and statistical isotropy of the observed field, we expect the two approaches to provide similar constraints. To show this is indeed the case, we have repeated the procedure of section III performing a Monte Carlo simulation over 1000 realizations in the ideal case of pure signal. The  $\chi^2$  using the cross spectrum  $C_l^{TC}$  can be calculated analytically by:

$$\chi^2(\Delta\alpha) = \sum (C_l^d - C_l^{TC})^2 / \sigma_l^2 \quad (11)$$

where as usual the prime identified rotated spectra, and the cosmic variance is given by [8] :

$$\sigma_l^2 = [(C_l^{TC})^2 + C_l^{TT} C_l^{CC}] / 2l + 1$$

and the maximum multipole in the sum is  $l_{max} \simeq 500$  roughly consistent with the maximum resolution employed in the wavelet analysis. In figure 4 we show  $\chi^2$  as a function of  $\Delta\alpha$  against the null hypothesis for wavelets and the cross spectrum  $C_l^{TC}$ . The two methods give very similar results, as expected in this ideal case.

#### IV. CONCLUSIONS

In summary, we have presented the first application of wavelets to polarized CMB maps, and used it to constrain the rotation angle of CMB photons in search of a signature due to cosmological birefringence, an effect connected to fundamental symmetry-breaking physics. We find no evidence of such a rotation and present the best upper limits to date on CMB data. This result should be compared with [21], where a marginal detection for a non-zero  $\Delta\alpha$  is claimed. The latter result is mostly based on the B03 data and only makes use of a subset of the WMAP3 dataset,

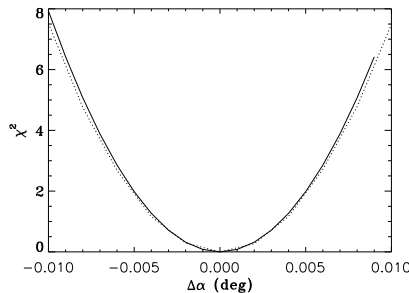


FIG. 4:  $\chi^2$  of the cosmological birefringence angle  $\Delta\alpha$  in case of pure signal using the wavelets estimator of the component TC (dotted) and the angular power spectrum  $C_l^{TC}$  (solid)

not including the  $TC$  correlations from which our results are essentially derived. While WMAP3 has lower signal to noise *per pixel* than B03, the analysis presented here uses data from  $\sim 60\%$  of the whole sky, while the limited useful sky coverage of B03 ( $\lesssim 1\%$ ) severely limits the statistical power of  $TC$ , so the detection in [21] appears to be driven from the much harder to measure (and prone to systematic effects)  $GC$  correlations<sup>2</sup>. Given the quantity and quality of the CMB data anticipated over the next few years, our approach demonstrates that substantially stronger limits on parity violation should be feasible.

## V. ACKNOWLEDGMENTS

We thank V. Antonuccio, O. Doré, M. Lattanzi and A. Palazzo for discussions. This research used resources of the NERSC, which is supported by the Office of Science of the U.S. DoE under Contract No. DE-AC02-05CH11231, and of the CASPUR supercomputing centre (Rome, Italy). Some of the results presented here have been derived using the Healpix package [36].

- 
- [1] Available from <http://lambda.gsfc.nasa.gov>
  - [2] D.N. Spergel *et al.*, *Astrophys. J.* in press, astro-ph/0603449.
  - [3] J. Kovac *et al.*, *Nature*, **420**, 772, (2002)
  - [4] A.C.S. Readhead *et al.*, *Science*, **306**, 836 (2004)
  - [5] F. Piacentini *et al.*, *Astrophys.J.*, **647**, 833, (2006); T.E. Montroy *et al.*, *Astrophys.J.* **647**, 813, (2006)
  - [6] B.R. Johnson *et al.*, astro-ph/0611394, (2006)
  - [7] L. Page, *et al.*, *Astrophys. J.* in press, astro-ph/0603450.
  - [8] M. Kamionkowski, A. Kosowsky and A. Stebbins, *Phys. Rev. D* **55**, 7368 (1997); U. Seljak and M. Zaldarriaga, *Phys. Rev. Lett.* **78**, 2054, (1997)
  - [9] R. Lenhert, hep-ph/0611177
  - [10] O.W. Greenberg, *Phys. Rev. Lett.* **89**, 231602 (2002); *Found. of Phys.*, **36**, 1535, (2006) (hep-ph/0309309)
  - [11] R. Bluhm, hep-ph/0112318; M. Mewes, hep-ph/0307161
  - [12] G. Amelino-Camelia *et al.*, *Nature*, **393**, 763 (1998)
  - [13] S.M. Carroll, G.B. Field & R. Jackiw, *Phys. Rev. D* **41**, 1231, (1990); S.M. Carroll & G.B. Field, *Phys. Rev. D* **43**, 3789, (1991)
  - [14] E.S. Scannapieco and P.G. Ferreira, *Phys. Rev. D* **56**, 7493 (1997)
  - [15] L. Pogosian, T. Vachaspati and S. Winitzki, *Phys. Rev. D* **65**, 083502 (2002); M. Giovannini, *Phys. Rev. D* **71**, 021301, (2005)
  - [16] A. Lue, L. Wang & M. Kamionkowski, *Phys. Rev. Lett.*, **83**, 1506, (1999); S. Saito, K. Ichiki & A. Taruya, arXiv:0705.3701, 2007

---

<sup>2</sup> Recently, Xia *et al.* [38] have extended the analysis in [21] including in their analysis the previously left aside WMAP3 full power spectrum dataset. They find  $\Delta\alpha = -6.2 \pm 3.8\text{deg}(1\sigma)$ , thus confirming a mild detection of a non-zero rotation angle. It would be very interesting to understand to what extent this is driven by the B03 dataset. An extension of our analysis to the B03 TQU maps (not yet public at the time of writing) is under study.

- [17] D. Maity, P. Majumdar, S. SenGupta, JCAP, 0406, 005, (2004); N.F. Lepora, gr-qc/9812077, 1998; K.R.S. Balaji, R.H. Brandenberger, D.A. Easson, JCAP, 0312, 008, (2003)
- [18] H. Davoudiasl *et al.*, Phys. Rev. Lett., **93**, 201301, (2004); H. Li, M. Li, X. Zhang, Phys. Rev. D **70**, 047302, (2004)
- [19] S. M. Carroll and G. B. Field, Phys. Rev. Lett., **79**, 2394, (1997); S. M. Carroll, Phys. Rev. Lett., **81**, 3067, (1998); B. Nodland, J.P. Ralston, Phys. Rev. Lett., **78**, 3043, (1997); D.J. Eisenstein, E.F. Bunn, Phys. Rev. Lett. **79**, 1957, (1997); J.P. Leahy, astro-ph/9704285, 1997
- [20] B. Feng, H. Li, M. Li, and X. Zhang, Phys.Lett. B **620**, 27 (2005)
- [21] B. Feng *et al.*, Phys. Rev. Lett. **96**, 221302, (2006)
- [22] M. Li *et al.*, hep-ph/0611192, (2006)
- [23] C. Q. Geng, S. H. Ho, J. N. Ng, arXiv:0706.0080, (2007)
- [24] V.A. Kosteletzky & M. Mewes, astro-ph/0702379
- [25] G. C. Liu, S. Lee and K. W. Ng, Phys. Rev. Lett., **97** 161303, (2006)
- [26] J.Q. Xia, H. Li, G.B. Zhao, X. Zhang, arXiv:0708.1111 (2007)
- [27] J. L. Sanz *et al.*, Mon. Not. R. Astr. Soc., **309**, 672, (1999)
- [28] L. Cayon *et al.*, Mon. Not. R. Astr. Soc., **315**, 757, (2000); L. Tenorio *et al.*, Mon. Not. R. Astr. Soc., **310**, 823, (1999); J. Gonzalez-Nuevo *et al.*, Mon. Not. R. Astr. Soc. 369 1603, (2006)
- [29] F.K. Hansen *et al.*, Astrophys. J., **648** 784, (2006)
- [30] D. Pietrobon, A. Balbi, D. Marinucci Phys. Rev. D **74** 043524, (2006)
- [31] P. Vielva *et al.*, Astrophys. J., **609** 22, (2004); M. Cruz *et al.*, Astrophys.J., **655**, 11, (2007)
- [32] P. Mukherjee & Y. Wang, Astrophys.J. **613**, 51, (2004); P. Cabella *et al.*, Mon. Not. R. Astr. Soc., **358**, 684, 2005
- [33] J.D. McEwen *et al.*, Mon. Not. R. Astr. Soc. Lett. **371**, L50, (2006)
- [34] E. Martinez-Gonzalez *et al.*, Mon. Not. R. Astr. Soc., **336**, 22, (2002); L. Cayon *et al.*, Mon. Not. R. Astr. Soc., **326**, 1243, (2001)
- [35] J.P. Antoine & P. VanderghEinst, J. Math. Phys., **39**, 3987, (1998)
- [36] K.M. Görski *et al.*, Astrophys. J., **622**, 759, (2005); web page: <http://healpix.jpl.nasa.gov>
- [37] N. Jarosik *et al.*, Astrophys. J. in press, astro-ph/0603452, (2006)
- [38] J. Q. Xia, H. li, X. Wang, X. Zhang, arXiv:0710.3325v1, (2007)